

Short-Range Correlations in Finite Nuclear Systems

Giampaolo Co'

Dipartimento di Fisica, Università di Lecce, and Istituto Nazionale di Fisica Nucleare sez. di Lecce, I-73100 Lecce, Italy

Abstract.

Recent results concerning the use of the Correlated Basis Function to investigate the ground state properties of medium-heavy doubly magic nuclei with microscopic interactions are presented. The calculations have been done by considering a Short-Range Correlation between nucleons. The possibility of identifying effects produced by Short-Range Correlations in electromagnetically induced phenomena is discussed.

1 Introduction

In many-body physics the word **correlation** indicates effects beyond Mean-Field (MF) theories. In nuclear physics it is common to distinguish between short- and long-range correlations. Nuclear collective phenomena such as vibrations and rotations are ruled by long-range correlations. These effects are well known and studied since the infancy of nuclear physics. On the contrary the study of the Short-Range Correlations (SRC) is a relatively new issue in nuclear physics. These correlations are produced by the strong repulsive core of the microscopic nucleon-nucleon interaction at short internucleon distances. In spite of the fact that all the microscopic nuclear theories need the SRC, clear signatures of their presence in medium-heavy nuclei have not yet been identified. The search for nuclear phenomena showing SRC effects is one of the most discussed topics of the last 15 years in the nuclear structure community.

In this contribution I shall be concerned about SRC. In the first part I shall present some results of microscopic calculations regarding ground state properties of medium-heavy nuclei. These calculations have been done with realistic nucleon-nucleon interactions and the SRC have been used to tame the repulsive

core of these interactions. In the second part of the contribution I shall discuss the results of a study aimed to identify the presence of SRC in nuclei by using experiments done with electromagnetic probes.

2 The Nuclear Ground State

The results presented in this section, have been obtained within the framework of the Correlated Basis Function (CBF) theory [1]. The starting point of this theory is the Ritz's variational principle:

$$\delta E[\Psi] \equiv \delta \left[\frac{\langle \Psi | H | \Psi \rangle}{\langle \Psi | \Psi \rangle} \right] = 0 \quad (1)$$

with the following ansatz for the many-body nuclear state:

$$|\Psi \rangle = F |\Phi_0 \rangle \quad (2)$$

where $|\Phi \rangle$ indicates a ground state Slater determinant constructed with a set of orthonormal single particle wavefunctions $|\phi \rangle$, and F is a many-body correlation function defined as:

$$F = \mathcal{S} \prod_{i < j} \left(\sum_{p=1}^n f^p(r_{ij}) O^p(i, j) \right) \quad (3)$$

In the above equation \mathcal{S} indicates a symmetrizer operator. The two-body correlation functions $f^p(r_{ij})$ have an operatorial dependence of the same type of that of the nucleon-nucleon interaction. In the present context I shall consider correlations up to $p = 8$ of the type:

$$O^{p=1,8}(i, j) = [1, \boldsymbol{\sigma}(i) \cdot \boldsymbol{\sigma}(j), S(i, j), \mathbf{L}(i, j) \cdot \mathbf{S}(i, j)] \otimes [\boldsymbol{\tau}(i) \cdot \boldsymbol{\tau}(j)] \quad (4)$$

where $S(i, j)$ is the usual tensor operator.

The problem is now well defined, and the minimization of the energy functional (1) is, at least in principle, only a technical matter. Monte Carlo techniques have been used [2] to solve the multidimensional integrals of eq. (1). This approach is *exact*, i.e. no further approximations are required, but it can be used only for relatively light nuclei. So far it has been applied to nuclei up to $A=8$, and for the ^{16}O nucleus the Monte Carlo calculations have been done with an approximation consisting in considering only up to four-body nucleon clusters [3].

It is clear that the minimization of the energy functional (1) for heavier nuclei requires the use of techniques alternatives to the Monte Carlo. These new techniques should simplify the problem by including new approximations. The idea is to find approximations affecting only irrelevant parts of the calculation, in order to obtain accurate results.

A technique rather well studied is the Fermi Hypernetted Chain (FHNC) theory [1], developed first for infinite systems such as liquid helium and nuclear matter. A first step in the application of the FHNC consists in a topological analysis of the various nucleon clusters formed by the interaction, by the SRC and by the antisymmetrization of the many-body wave function. It is possible to sum in a closed form all the diagrams with certain topological characteristics; these are called **nodal** diagrams. The other diagrams, named **elementary**, have to be calculated one by one, as in traditional perturbation theory. In this approach the most common approximation consists in neglecting the elementary diagrams. This approximation, called FHNC/0, is rather good in nuclear matter, even though it is not accurate enough for helium systems since they have a relatively higher density.

The FHNC theory has been extended to finite nuclear systems in refs. [4], and applied to light doubly magic nuclei in refs. [5,6] for simple interactions and correlations. The main goal of that investigation was a test of the validity of the theory. We found that the various sum rules were exhausted at the 0.1% level when a specific elementary diagram was included. We named this approximation FHNC-1.

Table 1. Binding energies per nucleon in MeV. The label *full* indicates that the minimization has been done on both correlation and single particle wave functions, while *corr* indicates that only the correlation has been varied.

^{16}O			^{40}Ca		
full	corr	exp	full	corr	exp
-5.48	-5.41	-7.97	-6.97	-6.64	-8.55

The next step of the work consisted in extending the theory in order to use realistic microscopic interactions with their full operatorial dependence. This requires to activate the analogous operatorial dependence of the correlation function, as given in eq. (3). The various terms of the correlation do not commute any more with the hamiltonian, and among themselves. The various cluster terms cannot be resummed in a closed form

For this reason it is necessary to introduce in the FHNC-1 computational scheme another approximation called Single Operator Chain. The FHNC-1 calculations in this approximation sum, in addition to all the nodal diagrams containing the scalar term of the correlation, only those diagrams where a single state dependent operator terms appears. This further approximation is slightly worsening the accuracy of the result. The sum rules are now exhausted at about the 5% level [7].

With this approach we have evaluated the ground state properties of the ^{16}O and ^{40}Ca nuclei using the realistic 2-body interaction Argonne V8' plus the 3-body Urbana IV force [8,9]. The first one is a reduced version of the Argonne

V18 interaction limited to the first 8 channels of eq. (4). In order to compensate for the truncation of 6 operatorial channel the parameters of the three-body Urbana IV force have been slightly readjusted [2].

The minimization procedure implied by eq. (1) involves both correlation and single particle wave functions. The energies obtained by this complete minimization are compared in Table 1 with the empirical binding energies. The discrepancy may seem rather large, but it is of the same magnitude of that of the best microscopic nuclear matter calculations.

The calculated charge densities distributions of ^{16}O and ^{40}Ca have been used to evaluate the elastic electron scattering cross section [8]. These cross sections are shown by the dashed lines of Figure 1 where they are compared with the data and the results of an analogous calculation done with the Argonne V14 interaction (dotted lines). Also in this case the agreement with the data is rather poor. Theory and experiments start to differ already at 30° .

The same computational scheme has been used by keeping fixed the set of single particle wave functions. We used a set already utilized in ref. [6] and chosen to reproduce charge radii and single particle energies around the Fermi surface. The minimum of the energy functional (1) is obtained by changing only the correlation. The results of this calculation are shown in Table 1 and in Figure 1 by the full lines.

The difference between the binding energies obtained with a full minimiza-

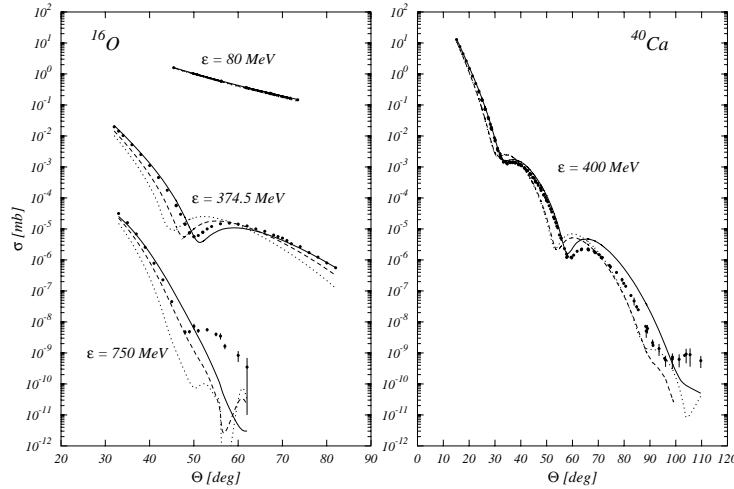


Figure 1. Elastic electron scattering cross sections. The full lines have been obtained with the empirical mean field wave functions and the V8' interaction. The dashed lines have been obtained by using the fully minimized densities with the V8' interaction and the dotted line with the Argonne V14 interaction.

tion and with the one restricted to the correlation function only, is of the order of the few percent. This seems to indicate the scarce sensitivity of this quantity to the single particle wave functions. On the other hand the charge densities, and consequently the cross sections, have been strongly modified. Now the agreement with the data extends up to about 60° .

This last set of single particle wave functions has been used to calculate the momentum distribution of the two nuclei considered [9]. The result of this calculation is shown in Figure 2. The dashed lines show the MF distributions, the dashed dotted lines have been obtained with purely scalar correlations and the full lines show the results of the complete calculation. These results show that the

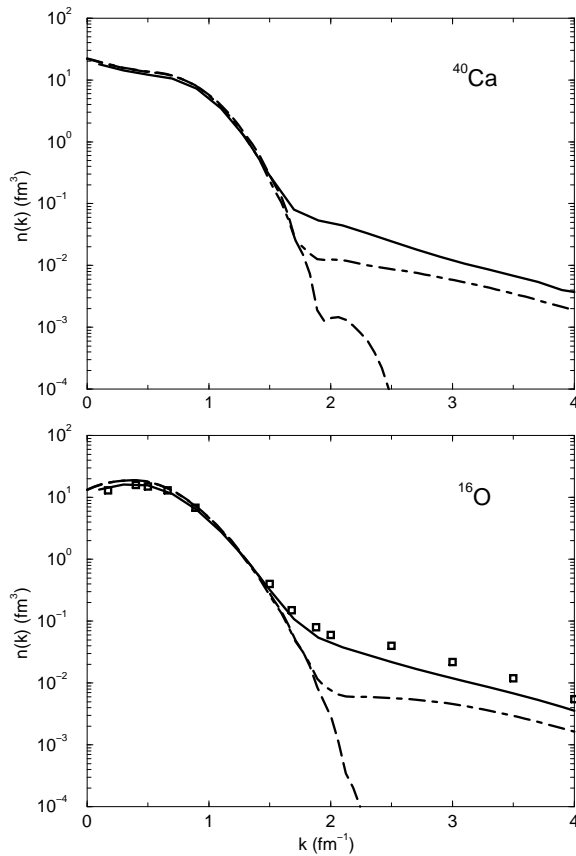


Figure 2. Momentum distribution. The full lines have been calculated considering central and tensor terms of the SRC. The dashed dotted lines have been calculated with only the central SRC and the dashed lines show the pure IPM results. The white dots are the Monte Carlo results of ref [3].

contribution of the state dependent terms of the correlation is not negligible. The agreement with the Cluster Monte Carlo momentum distribution of ^{16}O (white squares) is rather good.

The large increase of the correlated momentum distributions with respect to the MF results is a well known feature produced by the SRC [10]. Unfortunately the nucleon momentum distribution is not directly observable. It is therefore necessary to find observables related to it in order to identify the presence of SRC. This search should be done by studying the nuclear excited states. The results of this investigation are the subject of the next section.

3 Search for SRC Effects in Excitation Processes

In the framework of the CBF theory, the description of the excited states of the nucleus can be done by extending the ansatz of eq. (2):

$$|\Psi_n \rangle = F|\Phi_n \rangle \quad (5)$$

where now $|\Phi_n \rangle$ indicates a Slater determinant containing particle-hole excitations. In principle, in the description of the excited states also the correlation function should change, and the variational principle (1) should be again applied.

In reality, we have used the approach of Fantoni and Pandharipande [11] which considers both correlation function and MF potential fixed by the ground state minimization. The transition amplitude from the ground to an excited state, induced by an external operator, can be evaluated using cluster expansion techniques analogous to those used for the ground state. In the special case of infinite nuclear systems, it has been shown [11, 12] that it is possible to sum all the diagrams of a certain type.

Our calculations of the electromagnetic responses of finite nuclei, have an additional approximation, consisting in retaining only the diagrams that contain a single correlation line. This amounts to consider only certain classes of two-body and three-body cluster diagrams. As example I show in Figure 3 the Mayer-like diagrams considered in the case of an excited state which asymptotically can be described in terms of one-particle one-hole excitation. In ref. [13] this approximation has been tested against the complete calculation for the nuclear matter charge responses. The agreement between the two approaches is excellent. The differences are of the order of 10^{-5} .

The approach briefly outlined is reliable only to describe situations where nuclear collective effects are negligible. This means that the dynamics of the excitation should be dominated by single particle excitations.

For finite nuclear systems, the theory has been applied only for scalar correlation functions. Specifically we have used the single particle wave functions and correlations labelled S3 and V8 in ref. [6] and shown in Figure 4.

$$\begin{aligned}
 & \begin{array}{c} p \swarrow \quad \nearrow h \\ \blacksquare \\ (1.1) \end{array} + \frac{1}{2} \left[\begin{array}{c} p \swarrow \quad \nearrow h \quad i \\ \blacksquare \quad \cdots \quad \bullet \\ (2.1) \end{array} \quad - \quad \begin{array}{c} p \swarrow \quad \nearrow h \\ \blacksquare \quad \cdots \quad \bullet \\ (2.2) \end{array} \right. \\
 & \left. + \begin{array}{c} i \quad p \swarrow \quad \nearrow h \\ \bullet \quad \cdots \quad \blacksquare \\ (2.3) \end{array} \quad - \quad \begin{array}{c} h \swarrow \quad \nearrow i \\ \blacksquare \quad \cdots \quad \bullet \\ (2.4) \end{array} \right] \\
 & + \frac{1}{3} \left[\begin{array}{c} p \swarrow \quad \nearrow k \\ \bullet \quad \cdots \quad \bullet \\ (3.1) \end{array} \quad - \quad \begin{array}{c} p \swarrow \quad \nearrow k \\ \bullet \quad \cdots \quad \bullet \\ (3.2) \end{array} \right. \\
 & + \begin{array}{c} h \swarrow \quad \nearrow k \\ \bullet \quad \cdots \quad \bullet \\ (3.3) \end{array} \quad - \quad \begin{array}{c} h \swarrow \quad \nearrow k \\ \bullet \quad \cdots \quad \bullet \\ (3.4) \end{array} \right. \\
 & \left. + \begin{array}{c} h \swarrow \quad \nearrow p \\ \bullet \quad \cdots \quad \bullet \\ (3.5) \end{array} \quad - \quad \begin{array}{c} h \swarrow \quad \nearrow p \\ \bullet \quad \cdots \quad \bullet \\ (3.6) \end{array} \right]
 \end{aligned}$$

Figure 3. Mayer-like diagrams showing the two- and tree-body clusters terms included in the present work. The squares indicate the coordinate where the one-body electromagnetic operator acting on.

We first applied our model to high angular momentum stretched states in the discrete spectrum of ^{16}O , ^{48}Ca and ^{208}Pb [14]. Because of the high angular momentum these states are dominated by a single particle excitation. A typical result of this study is shown in Figure 5. The dashed lines represent the MF results while the full lines have been obtained by including the correlation terms of Figure 3. Clearly the SRC are unable to explain the quenching required to reproduce the experimental data.

We have applied our model in the quasi-elastic region for inclusive reaction [15]. Also in this case the excitation is dominated by one-particle one-hole exci-

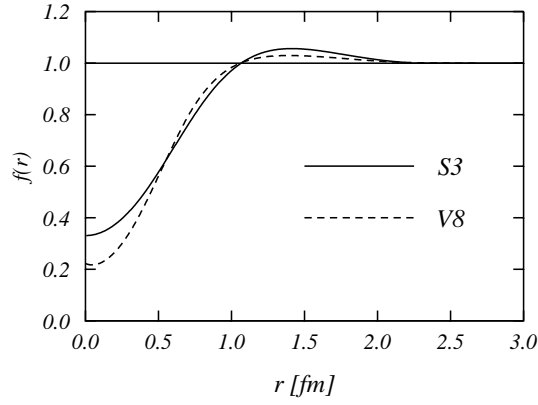


Figure 4. Two-body correlation functions used in the calculations of the electromagnetic response functions.

tation dynamics, therefore collective phenomena are negligible. However, contrary to the previous case, one has to consider the re-scattering of the emitted nucleon with the rest nucleus. This effect, usually named Final State Interaction (FSI), reduces the maximum values of the responses by a 20-30% factor [16].

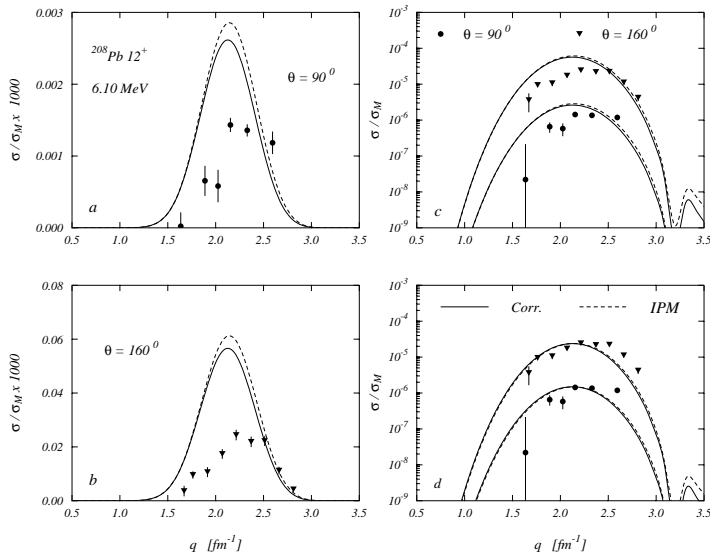


Figure 5. Inelastic scattering form factors calculated with SRC, full lines, and pure MF results, dashed lines. The left and right panels presents the same results in linear and logarithmic scale.

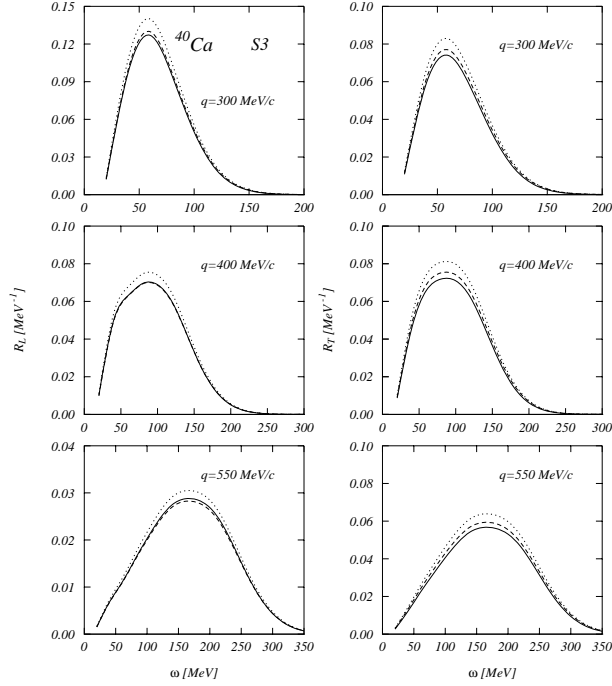


Figure 6. Charge, R_L , and current, R_T , inclusive responses. Full lines MF responses, dotted lines MF plus 2-point diagrams, dashed lines MF plus all the diagrams of Figure 3.

In Figure 6 we show the inclusive electromagnetic responses calculated in ^{40}Ca , without the inclusion of the FSI. The inclusion of only the 2-point diagrams of Figure 3 slightly increases the MF responses (full lines in Figure 6). The additional inclusion of the 3-point diagrams has an opposite effect with respect to that of the 2-point diagrams. The final difference between the MF and correlated responses is very small. The effect of the FSI is much larger than that of the SRC [15].

We have extended our model also to describe $(e,e'p)$ coincidence experiments on ^{16}O target [17]. To show the relevance of the 3-body cluster terms, I show in Figure 7 the normalized differences between the one-body response and the calculation considering two- and three body- SRC terms:

$$\Delta = \frac{R^{\text{CORR}}(|\mathbf{q}|, \omega) - R^{\text{MF}}(|\mathbf{q}|, \omega)}{R^{\text{MF}}(|\mathbf{q}|, \omega)_{\text{max}}} \quad (6)$$

The results of the two calculations presented in Figure 7 have been obtained with the correlations functions of Figure 4. Since the two correlations are rather

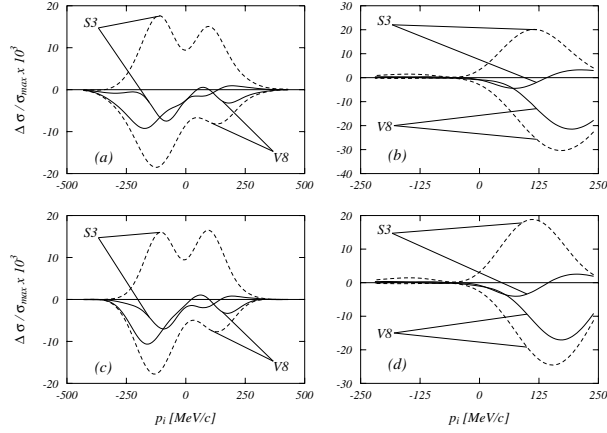


Figure 7. Normalized differences, eq. 6, calculated with the correlation functions of Figure 4. The dashed lines have been calculated by using two-point diagrams only, while the full lines show the inclusion of tree-point diagrams.

similar, it is plausible to expect that the results should not differ very much. This is not the case when only 2-point diagrams are used, as the dashed lines of Figure 7 indicate. The inclusion of the three-body clusters, which ensure the correct normalization of the nuclear final state, produces results which are rather similar for the two correlation functions.

The relevance of FSI is clear from the comparison with the ^{16}O NIKHEF data [18] shown in Figure 8. The full lines have been calculated without FSI and they are distant from the data points, while the dashed lines considering the FSI via optical potential are much closer. The SRC are unable to explain the need for a spectroscopic factor in order to reproduce the data, as the two lower panels clearly show.

Our model has been also applied to study nucleon emission induced by real photons. In Figure 9 I show some results of our investigation. The thin full lines have been obtained making a pure MF calculation with one-body current only. The inclusion of SRC, specifically the S3 of Figure 4, produces the dotted lines, while the inclusion of Meson Exchange Currents (MEC) gives the dashed lines. The thick full lines show the sum of all the effects considered.

The effect of the SRC seems to be relevant at high excitation energies and for large emission angles. Unfortunately also the MEC are important in this region, and they produce effects as large as those of the SRC, if not even larger.

We have applied our model to describe $(e,e'2p)$ processes [20]. In this case the MF responses induced by a one-body operator, which in the previous cases were giving the largest contribution to the cross section, are not present.

In Figure 10 the results for the ^{16}O $(e,e'2p)$ under the kinematics explained

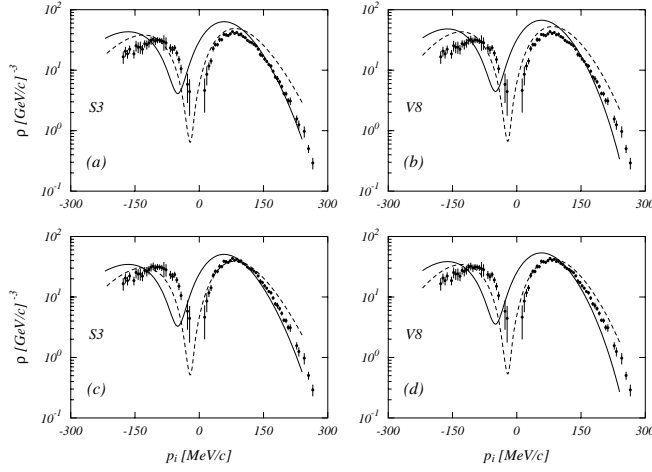


Figure 8. $^{16}\text{O} (e,e'p)^{15}\text{N}$ reduced cross section for the emission of the $1p1/2^{-1}$ proton calculated with the correlation functions of Figure 4. The full lines show the results obtained with a purely real MF basis, the dashed lines have been obtained with an optical potential. The curves in the lower panels have been produced by multiplying the upper curves with spectroscopic factor of 0.7.

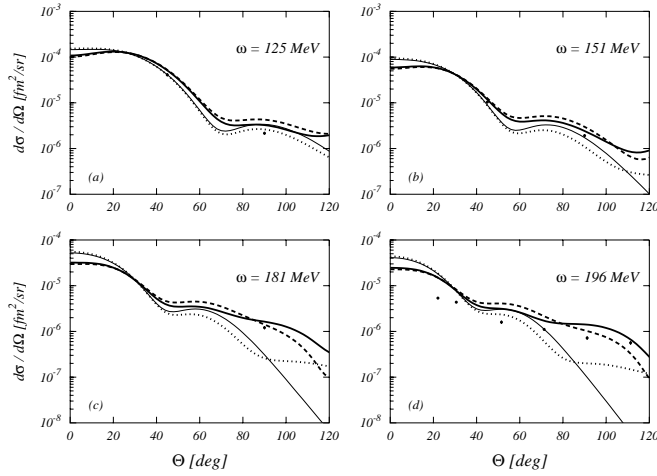


Figure 9. $^{16}\text{O} (\gamma,p)$ cross sections as a function of the nucleon emission angle for various values of the photon energies. The thin full lines show the MF results. The dotted lines include the effects of the S3 correlation. The dashed lines the MEC and the thick full lines all the effects.

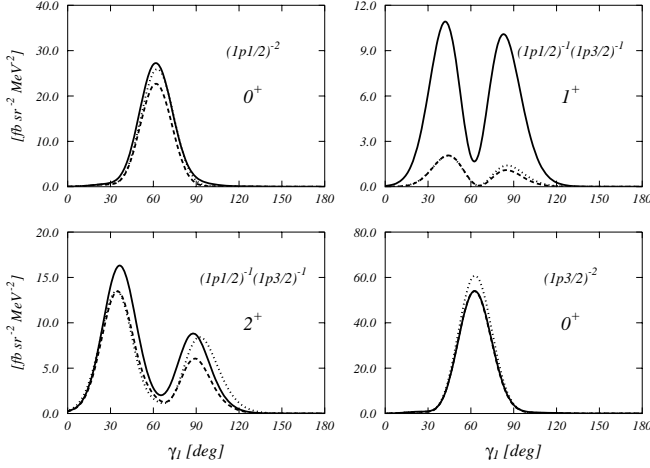


Figure 10. $^{16}\text{O}(e,e'2p)^{16}\text{O}$ cross sections as a function of the emission angle of one proton. The initial energy of the electron is 500 MeV, the nuclear excitation energy 200 MeV, the momentum transfer 300 MeV/c, and the second proton is emitted at 60° . The various labels in the figures indicates the single particle levels where the two protons are emitted and the angular momentum and parity of the residual A-2 nucleus. The dotted lines have been obtained with 2-point diagrams only, the dashed lines by adding the 3-point diagrams and the full lines consider also the contribution of the Δ excitation.

in the caption are shown. The dotted lines represent the results obtained by using only two-point diagrams, the dashed ones by adding the tree-body diagrams and the full lines include also the contributions of the excitation of the Δ resonance. It is interesting to notice the changes of the relative importance of the various components of the calculation by changing the nuclear final state. The common features of all the results shown in the figure is that the 3-point diagrams reduce the effect of the 2-point ones. This effect of the 3-point diagrams is consistent with all our previous calculations, and its physical origin is related to the correct normalization of the nuclear final state, as it has been detailed discussed in ref. [15].

Our calculation show that, even in this case, the contribution of the two-body currents, consisting here only in the Δ excitation term, may cover the SRC effects. The Δ excitation dominates the $(1p1/2)^{-2} 0^+$ and the $(1p1/2)^{-1} (1p3/2)^{-1} 1^+$ cross sections. In the other cases considered its effect is relatively small.

4 Conclusions

Microscopic calculations of nuclear properties require SRC to tame the strong repulsive core of the realistic nucleon-nucleon interaction. In our theory the SRC are an input fixed by the minimization of the hamiltonian expectation value.

Within our theory we succeeded in calculating the properties of ^{16}O and also of ^{40}Ca . The discrepancy with the empirical values of the binding energy is of the same amount of that of the best nuclear matter calculations. The value of this quantity shows a scarce sensitivity to the change of the single particle wave functions, contrary to the density.

To search for effects clearly produced by the SRC we developed a model describing nuclear responses. Within this model we have investigated the role of the SRC in (e,e') experiments both in the discrete and in the continuum spectrum. We have also investigated the single nucleon emission with both real and virtual photons. These processes are dominated by the MF transition densities, and the SRC produce very small effects. In specific situations when they show up, also the two-body MEC contribute, and the effects of these two processes strongly mix.

The two-nucleon emission processes are more promising, because in this case the MF contribution is absent. Also in this case the SRC effects fight against the MEC ones produced by the Δ excitation. On the other hand, the large number of variables could allow for the possibility of disentangling the two processes.

Acknowledgments

It is a pleasure to thank all the colleague and friends with whom I have worked on this project: J.E. Amaro, M. Anguiano, F. Arias de Saavedra, A. Fabrocini, S. Fantoni, P. Folgarait, I.E. Lagaris, A.M. Lallena, S.R. Mokhtar.

References

- [1] J.W. Clark, (1979) *Prog. Part. and Nucl. Phys.* **2** 89; S. Rosati, (1982) in *From nuclei to particles*, Proc. Int. School E. Fermi, course LXXIX, (ed. A. Molinari; North Holland, Amsterdam), p73.
- [2] B.S. Pudliner, V.R. Pandharipande, J. Carlson, S. C. Pieper and R. B. Wiringa, (1997) *Phys. Rev.* **C56** 1720; R. B. Wiringa, S. C. Pieper, J. Carlson and V.R. Pandharipande, (2000) *Phys. Rev.* **C62** 014001.
- [3] S. Pieper, R. B. Wiringa and V.R. Pandharipande, (1992) *Phys. Rev.* **C46** 1741.
- [4] S. Fantoni and S. Rosati, (1979) *Nucl. Phys.* **A328** 478; S. Fantoni and S. Rosati, (1979) *Phys. Lett.* **B84** 23.
- [5] G. Co', A. Fabrocini, S. Fantoni and I.E. Lagaris, (1992) *Nucl. Phys.* **A549** 439; G. Co', A. Fabrocini and S. Fantoni, (1994) *Nucl. Phys.* **A568** 359.
- [6] F. Arias de Saavedra, G. Co', A. Fabrocini and S. Fantoni, (1996) *Nucl. Phys.* **A605** 359.
- [7] A. Fabrocini, F. Arias de Saavedra, G. Co' and P. Folgarait, (1998) *Phys. Rev.* **C57** 1668.
- [8] A. Fabrocini, F. Arias de Saavedra and G. Co', (2000) *Phys. Rev.* **C61** 044302.
- [9] A. Fabrocini and G. Co', (2001) *Phys. Rev.* **C63** 044319.

- [10] A. N. Antonov, P. E. Hodgson and I. Zh. Petkov, (1988) *Nucleon Momentum and Density Distributions* (Clarendon Press, Oxford).
- [11] S. Fantoni and V. R. Pandharipande, (1987) *Nucl. Phys.* **A473** 234.
- [12] A. Fabrocini and S. Fantoni, (1989) *Nucl. Phys.* **A503** 375.
- [13] J.E. Amaro, A.M. Lallena, G. Co' and A. Fabrocini, (1998) *Phys. Rev.* **C57** 3473.
- [14] S.R. Mokhtar, G. Co' and A.M. Lallena, (2000) *Phys. Rev.* **C62** 067304.
- [15] G. Co' and A. M. Lallena, (2001) *Ann. Phys. (N.Y.)* **287** 101.
- [16] J. E. Amaro, G. Co' and A. M. Lallena, *Mean field description of electron induced quasi-elastic excitation in nuclei*, in *Quasielastic electron scattering in nuclei*, (R. Cenni Ed.; Nova Science).
- [17] S. R. Mokhtar, M. Anguiano, G. Co' and A. M. Lallena, (2001) *Ann. Phys. (N.Y.)* **292** 67.
- [18] M. Leuschner, J. Calarco, F.W. Hersman, E. Jans, G.J. Kramer, L. Lapikás, G. van der Steenhoven, P.K. de Witt Huberts, H.P. Blok, N. Kalantar-Nayestanaki, and J. Friedrich, (1994) *Phys. Rev.* **C49** 955.
- [19] M. Anguiano, G. Co', A. M. Lallena and S.R. Mokhtar, (2002) *Ann. Phys. (N.Y.)* **296** 235.
- [20] M. Anguiano, G. Co', A. M. Lallena, in preparation.